



This is a repository copy of *Short bursts of cyclic mechanical compression modulate tissue formation in a 3D hybrid scaffold.*

White Rose Research Online URL for this paper:
<http://eprints.whiterose.ac.uk/114887/>

Version: Accepted Version

Article:

Brunelli, M., Perrault, C.M. and Lacroix, D. (2017) Short bursts of cyclic mechanical compression modulate tissue formation in a 3D hybrid scaffold. *Journal of the Mechanical Behavior of Biomedical Materials*, 71. pp. 165-174. ISSN 1751-6161

<https://doi.org/10.1016/j.jmbbm.2017.03.008>

Article available under the terms of the CC-BY-NC-ND licence
(<https://creativecommons.org/licenses/by-nc-nd/4.0/>)

Reuse

This article is distributed under the terms of the Creative Commons Attribution-NonCommercial-NoDerivs (CC BY-NC-ND) licence. This licence only allows you to download this work and share it with others as long as you credit the authors, but you can't change the article in any way or use it commercially. More information and the full terms of the licence here: <https://creativecommons.org/licenses/>

Takedown

If you consider content in White Rose Research Online to be in breach of UK law, please notify us by emailing eprints@whiterose.ac.uk including the URL of the record and the reason for the withdrawal request.

Author's Accepted Manuscript

Short bursts of cyclic mechanical compression modulate tissue formation in a 3D hybrid scaffold

M. Brunelli, C.M. Perrault, D. Lacroix



PII: S1751-6161(17)30113-3
DOI: <http://dx.doi.org/10.1016/j.jmbbm.2017.03.008>
Reference: JMBBM2261

To appear in: *Journal of the Mechanical Behavior of Biomedical Materials*

Received date: 27 November 2016
Revised date: 7 March 2017
Accepted date: 8 March 2017

Cite this article as: M. Brunelli, C.M. Perrault and D. Lacroix, Short bursts of cyclic mechanical compression modulate tissue formation in a 3D hybrid scaffold, *Journal of the Mechanical Behavior of Biomedical Materials* <http://dx.doi.org/10.1016/j.jmbbm.2017.03.008>

This is a PDF file of an unedited manuscript that has been accepted for publication. As a service to our customers we are providing this early version of the manuscript. The manuscript will undergo copyediting, typesetting, and review of the resulting galley proof before it is published in its final citable form. Please note that during the production process errors may be discovered which could affect the content, and all legal disclaimers that apply to the journal pertain

Short bursts of cyclic mechanical compression modulate tissue formation in a 3D hybrid scaffold

M. Brunelli¹, C.M. Perrault², D. Lacroix^{2*}

¹EMPA, Swiss Federal Laboratories for Materials Science and Technology, Lerchenfeldstrasse 5, 9014 St. Gallen, Switzerland

²INSIGNEO Institute for in silico medicine, Department of Mechanical Engineering, University of Sheffield, UK

*Corresponding author. Damien Lacroix Department of Mechanical Engineering F32, Pam Liversidge Mappin Street Sheffield S1 3JD Tel.: +44(0)114 2220156; d.lacroix@sheffield.ac.uk

ABSTRACT

Among the cues affecting cells behaviour, mechanical stimuli are known to have a key role in tissue formation and mineralization of bone cells. While soft scaffolds are better at mimicking the extracellular environment, they cannot withstand the high loads required to be efficient substitutes for bone in vivo. We propose a 3D hybrid scaffold combining the load-bearing capabilities of polycaprolactone (PCL) and the ECM-like chemistry of collagen gel to support the dynamic mechanical differentiation of human embryonic mesodermal progenitor cells (hES-MPs). In this study, hES-MPs were cultured in vitro and a BOSE Bioreactor was employed to induce cells differentiation by mechanical stimulation. From day 6, samples were compressed by applying a 5% strain ramp followed by peak-to-peak 1% strain sinewaves at 1 Hz for 15 min. Three different conditions were tested: unloaded (U), loaded from day 6 to day 10 (L1) and loaded as L1 and from day 16 to day 20 (L2). Cell viability, DNA content and osteocalcin expression were tested. Samples were further stained with 1% osmium tetroxide in order to investigate tissue growth and mineral deposition by micro-computed tomography (μ CT). Tissue growth involved volumes either inside or outside samples at day 21 for L1, suggesting cyclic stimulation is a trigger for delayed proliferative response of cells. Cyclic load also had a role in the mineralization process preventing mineral deposition when applied at the early stage of culture. Conversely, cyclic load during the late stage of culture on pre-compressed samples induced mineral formation. This study shows that short bursts of compression applied at different stages of culture have contrasting effects on the ability of hES-MPs to induce tissue formation and mineral deposition. The results pave the way for a new

approach using mechanical stimulation in the development of engineered in vitro tissue as replacement for large bone fractures.

1 Introduction

In early studies the effect of mechanical forces on cell response was mainly investigated on 2D substrates [1]–[4], the geometry of which was not a good representation of the 3D architecture of biological tissues. The increasing demand for a structure that matched the architecture and chemistry of injured sites led to the development of 3D scaffolds [5]. Among those, hydrogels were shown to enhance cell survival and provide a tissue-like environment for cell growth and differentiation [6]. Moreover, they offered a compact matrix, often made of proteins, which guaranteed uniformity of stresses when mechanical forces were applied. However, the application of such scaffolds are limited by their soft matrix, preventing their use when they are required to bear high stresses [7], such as those acting on bone. As a consequence, the focus moved toward the use of 3D polymeric structures able to bear mechanical loading [8], [9]. Scaffolds made by polymerization of polylactic acid, polyglycolic acid or polycaprolactone (PCL) were widely investigated because they are easy to shape through high-temperature processes, allowing the fabrication of highly reproducible fibrous structures [10]. Despite their remarkable resistance to forces, 3D polymeric scaffolds are not a good reproduction of the mechanical environment found in tissue. Indeed, the stresses felt by cells following the compression of such structures are limited to the 2D surface of cellular adhesion. In order to increase the three dimensionality of the constructs and obtain a more realistic reproduction of the in vivo environment, we propose a new hybrid scaffold composed of stiff 3D PCL and a soft collagen matrix with the aim of providing a uniform distribution of stresses surrounding cultured cells.

Mechanical differentiation of cells has mainly been investigated using hydrogels [11], [12], 2D substrates [13], [14], or 3D foam-like scaffolds [15]. In general, high-amplitude compression strains applied to scaffolds with embedded cells have shown to induce chondrogenic differentiation [12], [16]–[18], while tensile stimuli with frequencies mimicking those forces affecting bone in vivo have been shown to induce osteogenic differentiation on 2D substrates [3], [4], [19], [20]. Compression of scaffolds was also found to enhance osteogenesis on 2D [3] as well as 3D structures [21], if the force was applied for short periods of time. The inclusion of resting periods of 5 days among stimulations in combination with short bursts of compression was also found to induce mineral production on differentiated osteoblasts [15]. Despite numerous studies on the topic, none have focused on the potential of serial cyclic stimulations in inducing mineralization of undifferentiated cells. For this purpose, this study aims to elucidate how short bursts of compression applied to 3D scaffolds embedding collagen and cells, and the repetition of the stimuli at late stage of culture affect 1) hES-MPs proliferation; 2) spatial formation of extracellular matrix (ECM) and mineral deposition; and 3) osteogenic protein expression. Moreover, techniques commonly used to assess cell activities, such as assays quantifying metabolic activity, cell number and protein expression, are used alongside x-ray scanning to determine the distribution of collagen, cells, ECM and mineral through the whole structure.

2 Materials and methods

2.1 Mechanical relaxation of PCL

3D Insert PCL scaffolds (Biotek, USA) were initially mechanically relaxed at 37°C by applying a 8% strain compressive ramp calculated over the height of the sample. Any stress from the structure was removed by maintaining a constant displacement for 180 min [22].

2.2 Scaffold sterilization and hES-MPs seeding

The surface of the scaffolds was activated by applying air plasma treatment (Diener, Germany) for 5 minutes at 30 W and 1 mBar. Samples were then sterilized by alternating a washing process involving 70% ethanol and PBS three times. Eventually, samples were let to dry for 30 minutes under a biological hood and seeded with human embryonic stem cell-derived mesodermal progenitors (hES-MPs). Bovine collagen type 1 (Gibco, UK) was diluted to a concentration of 2 mg/ml with 0.1M NaOH, 1% PBS and α -mem culture media (SLS, UK) supplemented with 10% FBS (Labtech, UK), 1% penicillin/streptomycin/L-glutamine (SLS, UK) [23]. hES-MPs (passage 5) were included in the solution to obtain a final concentration of 2×10^6 cells/ml. Samples (N=36) were then statically seeded by depositing a drop of 20 μ l of collagen/cells solution on the top surface of scaffolds. Such a seeding density was chosen because previous studies showed a tendency toward osteogenic differentiation [26], [27]. hES-MPs were used as the cell source because of their reduced risk of tumour development due to the fact that their differentiation pathway is already partly defined and because they are expected to be more stable compared to other type of highly proliferative lineages such as embryonic stem cells enabling future therapeutic applications and advantages for bulk production of cells for therapy [24]. hES-MPs led to an higher production of tissue formation compared to adult mesenchymal stem cells when culture in column bioreactors showing great potential for the development of bone substitutes [25]. Scaffolds were kept in culture during the whole experiment using the same media formulation used for the dilution of the collagen.

2.3 Mechanical compression of seeded cPCL

3D Insert PCL scaffolds (Biotek, USA) were divided in groups depending on the mechanical protocol to be applied. A total of 48 samples were used in each experiment: 18 were kept in free-floating conditions, 18 were cyclically loaded and 12 were kept as controls with collagen but without cells in free floating conditions. After 5 days in culture to allow the adaptation of cells to the environment, samples were collected and placed into a previously autoclaved biodynamic chamber (Fig. 1) for compression. The chamber was then mounted onto a bioreactor (BOSE Electroforce, USA) and a preload of 0.1 N was applied to avoid shifting of the specimen. The chamber was then filled with media by pumping the fluid with a peristaltic pump and samples underwent cyclic compression (Fig. 2):

- 1) superimposing a 5% strain ramp at 10 μ m/s;
- 2) applying a 2% peak-to-peak (from 4 to 6% strain) sinusoidal waveform at 1 Hz for 15 min;
- 3) removing the superimposed ramp by unloading the sample at 10 μ m/s.

The chamber was then removed from the bioreactor, placed under a culture cabinet, and samples were moved to 96 well plates with culture media. The latter was changed every day with 200 μ l of new culture media. Non-loaded samples (U) were kept in static culture and no compression was applied. The response of cells cultured in non-loaded samples was compared with samples loaded for 15 min per day (Table 1), from day 6 to day 10 (L1). Half L1 samples were then compressed again from day 16 to day 20 (L2).

2.4 Analysis of hES-MPs response

Time points were set at 1, 3, 7, 14, 21 and 28 days and the initial number of samples varied among conditions. At day 1 and day 3, no samples had undergone compression (Fig. 3), therefore testing three random samples over the entire batch provided a good representation of the behaviour of cells for all samples involved in the experiment. At day 7 and 14, samples were either non-loaded or loaded with a single series of cycles and therefore a total of six samples needed testing, three for each condition.

The last time points were preceded by a second series of compression cycles, therefore nine samples were tested at day 21 and 28. Thus, at day 0 (Table 1):

- 18 samples accounted for U as 3 samples were tested at each time point ($3 \times 6 = 18$);
- 12 samples accounted for L1 as 3 samples were tested at day 7, 14, 21 and 28 ($3 \times 4 = 12$);
- 6 samples accounted for L2 as 3 samples were tested at day 21 and 28 ($3 \times 2 = 6$).

The entire experiment, from day 1 to day 28, was repeated three times to assess reproducibility and any variability due to slightly different external conditions and scaffolds architecture. The number of samples, involved in Presto Blue (Table 3) or other assays (Table 2), enabled statistical analysis. For each condition, a minimum of three samples were considered, averaging values from the three repeats of the experiment. Data were tested for normality and equality of variances by Shapiro and Levene's test respectively, but due to the high variability between series, Games-Howell non-parametric test was also applied.

2.5 Viability assay

Presto Blue (Presto Blue™ Cell Viability Reagent, Gibco) was performed on samples fitted in a 96 well plate and previously washed with PBS. Briefly, 200 μ l of Presto Blue (1:10 v/v in culture media) was added to samples and left to react for 1 hour in an incubator. Viability was assessed by withdrawing 180 μ l of fluorescent solution from each well and reading fluorescence by microplate reader at ex/em 540/590 nm.

2.6 hES-MPs response to compression

Before performing any further analysis, the equality of samples belonging to different groups (U, L1, L2), but undergoing the same protocol (Fig. 3), was tested at each time point by Presto Blue. A variable number of samples was considered due to the sacrifice of three samples at each time point

(Table 3). The number of samples tested by Presto Blue differed up to day 21, as U and L1 were tested for a higher number of time points (Fig. 3).

2.7 DNA and osteocalcin ELISA assay

Two samples were collected at each time point and DNA was quantified by Quant-IT DNA kit (Gibco, UK). Briefly, samples were cut into pieces and immersed in 200 μ l of 0.5% trypsin for 5 minutes. Then, 200 μ l of culture media was added and samples were vortexed for 5 s. 20 μ l of suspension was diluted in DNA lysis buffer (distilled water, 1Mm magnesium chloride, 5 mM calcium chloride, 1% Triton X, 10% Tris-EDTA) and picogreen stain (200:1 v/v) was added. Fluorescence was read at 485/535 nm after 30 minutes. The remaining solution was stored at -80°C for osteocalcin (OCN) quantification by ELISA assay (CytoSet kit, Life Technologies, UK). At each time point, a control sample was collected for DNA assay and, then, was stored in the same conditions as samples for OCN ELISA.

2.8 Osmium staining and micro computed tomography

At each time point, a sample was fixed with 180 μ l of 2.5% glutaraldehyde for 2 hours, and then 20 μ l of osmium tetroxide was added and left to react overnight. Samples were washed 3 times with distilled water and then allowed to air dry. All samples were scanned with SkyScan 1172 (Bruker, Belgium) at 40KV, 255mA and 10W within 3 days of staining. Pixel size was set at 17.4 μm and images were reconstructed by the CTAn reconstruction software (Bruker, Belgium) accounting for ring artefacts and beam hardening correction of 10% and 15% respectively. A control sample underwent osmium staining and x-ray scanning to account for the initial injection of collagen gel.

2.9 Segmentation

2D Images were segmented by ScanIP (Simpleware Ltd., UK) and 3D structures were analysed to quantify mineral, and tissue formation. As the intensity of the signal from the x-ray is related to the density of the scanned material, signal in the low (3,500-7,500) grey values (GV) range was considered to be volumes of tissue occupied by cells and ECM (Fig. 4). Higher GV (13,000-60,000) were instead attributed to the mineral phase (Fig. 4). Values between 7,500 and 13,000 were associated to with the scaffolding structure. The amount of tissue and mineral was further divided, among material developing on the surface or in the internal volume of the scaffold, through selection of a region of interest (ROI) with cylindrical shape measuring 4 mm in diameter, 0.5 mm in height and concentric to the scaffold. All the values were calculated subtracting the volume of tissue or mineral of each condition to the volume of collagen detected in the controls at the same time point.

2.10 Fluorescent staining and cellular apoptosis

Cellular apoptosis was evaluated by fluorescent imaging. At day 28 samples were collected and washed with 200 μ l PBS. After addition of 200 μ l of fluorescent stain made of 2 μM Calcein AM (Gibco, UK) and 4 μM Ethidium bromide (Sigma Aldrich , UK) in PBS, samples were kept in an incubator covered in aluminium foil. After 30 minutes, Samples immersed in PBS were imaged by

fluorescent microscopy and pictures were elaborated by the Metamorphosis software (Nikon, Japan). The time of exposure was set to:

- Blue light (scaffold autofluorescence): 40 ms;
- Red light (dead/apoptotic cells): 40 ms;
- Green light (alive/viable cells): 200 ms;

and reconstructed by ImageJ (NIH, USA).

3 Results

3.1 hES-MPs viability

At day 1 and 3 cells were shown to be viable and samples from different groups had similar fluorescent values, (Fig. 5). After one day of stimulation (day 7), the fluorescent signal of loaded samples was weaker compared with free-floating samples, although cell metabolic activity increased for both conditions. Between day 7 and day 21, the metabolic activity remained unvaried among time points as well as loaded and non-loaded samples. Due to the high standard deviation, no significant differences among conditions were identified by statistical analysis at any time point, except at day 28 when non-loaded samples underwent a further increase in cellular metabolism. Similar results were obtained by fluorescence images taken at each time point (Fig. 6). A lower green signal was characteristic of scaffolds undergoing compression at both day 7 and day 28. At the latter time point, cells were well elongated and spread in all cases, but clear signs of proliferation were mainly observed on non-loaded conditions where cells covered the entire surface of the scaffold. Cells appeared to align in the same direction, developing a highly interconnected cellular network in U and L1. On the contrary, cells embedded in samples undergoing twice the cyclic loading appeared less oriented, with thin protrusions spreading in different directions and conferring a more star-like shape (Fig. 6).

3.2 hES-MPs proliferation and ECM production

The proliferation of cells was quantified by DNA assay (Fig. 7). An increase in cell number was observed at day 14 for U ($p<0.05$), and day 21 for L1 ($p<0.05$) and L2 ($p<0.05$). However, L2 showed lower cell content compared with L1 at every time point ($p<0.05$), and a decrease in cell number occurred at day 28 for all tested conditions. A similar trend was observed by considering the x-ray signal (Fig. 8). Cellular content began to be detected from day 3 when cells assumed a more elongated shape and produced ECM. Tissue content experienced a decisive increase at day 21 for all conditions, although an earlier increase in cell proliferation for U was already observed at day 7. However, the enhanced decrease in cellular content was not observed for L2 at day 28, contrasting with the DNA results. The growth of tissue was mainly enhanced on the surface of scaffolds with no differences among loading conditions within the first 14 days of culture (Fig. 9). Small differences were instead detected in internal ROI where the average tissue volume amounted to $40\pm 12\%$, $45\pm 7\%$ and $47\pm 8\%$ respectively for U, L1 and L2 samples over the entire duration of the experiment.

From day 21, tissue growth involved volumes either inside or outside the ROI for L1, followed by a quick drop in tissue content at day 28.

3.3 Mineralization

Further observation of μ CT scans allowed the isolation of the signal from the mineral formed by the action of cells by selecting high intensity GV (Fig. 10). U samples mineralized at day 14 and the mineral content remained constant for the remainder of the experiment. On the surface mineral content was 2 mm^3 , but it was below 0.5 mm^3 in the internal volume, close to the detectable threshold. By contrast, cells in loaded samples started to produce mineral inside the ROI as well as on the surface from day 7, suggesting an early mineralization process triggered by the cyclic load applied. Although the early mineralization response triggered in L1 samples was not observed in free-floating conditions, U samples showed a 6-fold higher volume of mineral compared with L1 from day 14 onwards, suggesting that cyclic load prevented mineralization when applied at the early culture stage. The load elicited a strong effect on mineralization also when applied at the advanced culture stage. Indeed, L1 samples did not show any further sign of mineralization after day 7, and the mineral phase at day 28 was only 25% of the amount detected in U. Conversely, a second series of compression cycles enhanced mineralization at day 21, and the mineral content became a significant 30% higher at day 28 compared with U ($p < 0.05$). Moreover, the mineralization in ROI for L2 (Fig. 11) was 3-fold higher than the other tested conditions from day 21, suggesting late cyclic stimuli to induce mineralization on previously compressed samples. The pattern of mineralization observed by μ CT was confirmed by quantification of OCN by sandwich ELISA (Fig. 12). Although not statistically significant, OCN was expressed on L1 samples at day 7, suggesting the possibility of an early cellular response triggered by the mechanical loading. Moreover, the effect of cyclic loading, applied at the later stage of culture on the mineralization potential of cells was further confirmed at day 28 by the significantly higher ($*p < 0.05$) amount of OCN expression detected in L2 samples compared with U and L1. The total amount of osteocalcin for U, L1, and L2 at day 28 was 35.1, 28.3 and 35.9 pg respectively.

4 Discussion

4.1 Mechanical compression and proliferative response

3D PCL was shown to be suitable for prolonged culture of cells and for promoting the proliferation of hES-MPs in the scaffold. In fact, Presto Blue gave a good insight into the behaviour of hES-MPs, however only for those located at the surface of the sample due to limitations related to: 1) the porosity of samples preventing the complete washout of the fluorescent solution from the internal volume; and 2) the development of an external layer of cells, blocking the diffusion of molecules in the interior of the structure. Despite this, Presto Blue was used to confirm equality among samples in terms of initial number of embedded cells and as an indication of the cellular metabolic activity. As a consequence, any difference in the cellular response could be related to the applied mechanical conditions rather than initial differences among samples. Specimens assigned to different groups (e.g. L1 and L2) underwent the same mechanical stimulation at early time points (e.g. day 7 and 14).

As a consequence, if Presto Blue gave the same fluorescence signal for all samples, they were considered as belonging to the same group. Indeed, the L2 condition appears just after day 21 when some of the samples from L1 were taken and underwent further stimulation at day 21 and 28. A reliable proliferation profile was provided by quantification of DNA content.

In contrast to Presto Blue, DNA quantification required the destruction of the sample, enabling the complete extraction of cells and providing information on cells located in the internal volumes of samples. DNA assay is a highly sensitive test and provided precise measurements with standard deviations below the 30% of the average values except for loaded samples at day 28. The high standard deviation observed at the end of the experiment can be explained by differences among the repeats - in terms of initial concentration of collagen, scaffold geometry, and slightly different media formulations - which progressively affect the behaviour of cells over time and become more evident at later stage of culture. According to DNA quantification, cyclic compression applied over 5 days caused a delayed proliferation compared with the other tested conditions. On the contrary, L2 samples did not show any sign of proliferation after 5 days of rest, suggesting that 1) cyclic compression of scaffolds over a 5 day-length period induces proliferation only if the stimulus is applied once; 2) equally long resting periods are not enough to recover from the previous series of compression cycles and enhance proliferation; and 3) a second series of cyclic compression further delays or may block proliferation, although enhancing ECM and mineral production. Whether a second series of cyclic compression causes delay or blocks the proliferation of cells can be clarified by performing longer experiments, testing samples at day 31, at least, to equalize the time elapsed between loading series. However, comparison with the other loading conditions could be difficult due to the progressive apoptosis already observed at day 28 for U and L1 samples (Fig. 13).

Improved proliferation after cyclic load was also claimed in the literature, although different scaffolds, compression protocols, and cell type were employed. For example, murine embryonic stem cells seeded in collagen type 1 scaffolds and compressed 4 hours a day presented higher viability over time compared with non-loaded samples [28]. Enhanced variability associated with daily compression of 3D samples was also observed in other studies on hES-MPs seeded, bone-mineralized scaffolds [29].

4.2 ECM deposition and tissue development

A proliferation profile similar to DNA was obtained from the reconstruction of μ CT images. Further differentiation between tissue and mineral formation was performed by splitting the signal among different densities. Tissue content was related to a less dense material associated with growth of cells and ECM deposition. Observing the growth of tissue in the internal volume of samples, the high variability up to 12% in U is likely to reflect the differences in porosity among samples. Indeed, diffusion of molecules is expected to be facilitated through larger porous samples, enhancing cell survival. A less variable and higher percentage of viable cells was found in the inner volumes of loaded samples, suggesting a possible involvement of cyclic load in the mass transport of nutrients throughout the structure. As a result of cyclic deformation, a gradient of pressure is believed to arise, enhancing convective transport of fluid and cell survival through the whole structure. At day 21, the absence of proliferation detected in L2 confirmed prolonged cyclic load to prevent proliferation.

At day 28 all conditions showed cellular apoptosis (Fig. 13), which is believed to be associated with a lack of nutrients in the interior regions of samples because of the development of the external layer. A decrease in tissue content was also observed on the surface of L1 samples, suggesting the occurrence of a programmed cell death phenomenon due to the high density achieved [30], [31] at day 21.

Differences in cell quantification among DNA and μ CT may be related to the production of ECM, the signal for which is accounted for during μ CT reconstruction while being excluded in the DNA quantification. Splitting the signal coming from cells and ECM into two separate components was impossible due to the type of contrast agent employed in the study, presenting the same absorbability to cells and ECM. Following this observation, the absence of a decrease in tissue volume in L2 between day 21 and day 28, can be reasonably associated with matrix production as well as variations in cell number. Increased production of ECM as a consequence of short bursts of compression was also claimed in another study [21] where hES-MPs seeded on polyurethane scaffolds underwent stimulation at 5% global strain for 2 hours. Similarly to our study, resting periods of 5 days were allowed between series of compression.

4.3 Tissue and mineral growth

Cyclic loading affected proliferation, tissue formation, cell survival, as well as mineralization potential of cells. Mineralization occurred and was observed as appearance of a more dense material into the scaffold, linked to the deposition of salt crystals. At day 7, an early sign of mineralization was observed in loaded samples and confirmed also by OCN quantification. However, the early presence of mineral content and the mechanism governing such activation needs to be further clarified and confirmed due to the high standard deviation associated with both measurements. In general, no degradation of the mineral content was observed over long periods of time (Fig. 14). Indeed, U increased the mineral volume up to 2 mm³ in the first 14 days, L1 showed a slight sign of mineralization at day 7 and L2 reached the highest mineral content of 3 mm³ after 21 days. However, the amount of mineral remained constant until day 28 for all conditions. The mineral content increased without ongoing proliferation which suggests a strong link between the two processes, the turnover of which is largely affected by the mechanical cues provided by the surrounding environment. Such a hypothesis is supported by the literature showing that genes expressed during proliferation (e.g. FGF-2) are instead downregulated during mineralization and vice versa (e.g. BMP-2)[32]. Applying a load at day 6 seemed to enhance mineralization and to temporarily decrease the proliferation potential of cells. At the same time, it seems to have postponed tissue growth as noticed for L1 at day 21, while further delaying the mineralization which may occur after day 28. Unfortunately, longer studies, not involving compression of samples, are difficult to perform due to the increased cellular death observed after 28 days in culture. As explained earlier, this is probably due to the high proliferation rate of cells in contact with constantly accessible nutrients and gasses at the surface creating a barrier to diffusion, as well as the production of ECM reducing the diffusion capability of the matrix. It is interesting to note that, similar studies have reported an increase in calcium or OCN content as consequence of cyclic compression of scaffolds. For example, expression of OCN was noticed on cells cultured on 2D substrates which underwent continuous strain over 14 days [1]. Mineralization in terms of calcium

deposition and bone volume was shown to be elicited on 3D scaffolds by using relatively short bursts of compression both in vitro [15], [33] as well as in vivo [34], [35].

4.4 Mechanical differentiation of hES-MPs in cPCL

The shape of cells at day 28 excluded differentiation toward the chondrogenic pathway, as in all cases cells were well elongated with extended protrusions rather than spherical. Loaded samples exhibited a less compact tissue-like organization on the surface compared with non-loaded samples probably due to the repetitive contact between the sample surface and the bioreactor shafts, causing slight damage to the most exposed tissue. Moreover, L2 cells appeared star-like, with multiple, randomly oriented, thin protrusions. These findings, together with the volume of mineral found by x-ray scanning and the expression of osteocalcin detected for L2 at day 28 may be sign of osteogenic differentiation. This contradicts previous reports, in which 2D substrates [1]–[4] showed enhanced osteogenesis with applied tensile strains but chondrogenesis with applied compression [12], [17], [18], [36]. On the contrary, mineralization occurred in this study as a consequence of compression of scaffolds. This discrepancy in the literature is probably due to the different type of scaffolds considered. Indeed, 2D substrates transmit stresses to cultured cells only through the attachment surface while hydrogels provide a different distribution of stresses through space compared with that elicited by the cPCL structure due to their soft and compact matrix. Another key difference between 2D substrates and cPCL concerns the distribution of stresses. Indeed, diverse stresses act throughout the structure because of irregularities in the geometry of fibers and also the presence of collagen further increases the variability in the mechanical environment surrounding the cells. To date, local tensile stresses were shown developing from the compression of 3D PCL [37] while further clarification of the deformations affecting collagen is required to understand the link between the cellular response obtained in this study and the mechanical forces sensed by cells. According to other studies where load was applied to 3D scaffolds by four-point bending devices, compression of scaffolds could elicit a decrease in the chondrogenic potential of cells [38] and enhance osteogenic differentiation [29], [39]. However, the different type of cells and the different loading protocols applied in the experiments do not allow a direct comparison with those studies. The response to mechanical stimuli, as well as other environmental cues, are strongly linked to the cell lineage, and cells are highly sensitive to a number of factors in mechanical stimulation, such as the amplitude, frequency, the day stimulation begins, and the duration of the stimuli, leading to different responses. For example, polyurethane scaffolds showed enhanced chondrogenesis on hES-MPs for high strain above 10% [16], while more moderate strains below the 10% enhanced matrix production on hES-MPs [15] and mineral deposition on MLO-A5 [21].

5 Conclusions

This study highlights how a composite scaffold combining the mechanical strength of PCL and the soft nature of hydrogels is particularly adequate to perform mechanical stimulation of cells over long periods of time (28 days). A unique characteristic of this study is the special attention taken to ensure repeatability in the mechanical stimulation despite the substantial architectural differences in the PCL scaffold. Cell behaviour was evaluated across the overall amount of material in the sample

without distinguishing among local stress variation, geometrical differences or imperfections. As a consequence, the variability of the experiments is increased as differences in local geometry produce variation in the distribution of local stresses and to the stimuli applied to cells. As the same trend, with regards cellular response was observed regardless the differences among scaffolds, a stronger association is believed to exist between the applied compressive protocol and the overall cellular response obtained. Scaffolds undergoing short daily bursts of compression showed variations not only in terms of proliferation but also in the mineralization potential of cells. Particularly interesting was the dual effect of compression in enhancing proliferation and preventing mineralization if applied at an early stage of culture or, vice versa, suppressing proliferation and promoting mineral deposition if repeated after 5 days. This study introduces a new experimental approach for inducing mineralization of undifferentiated cells which could have great potential in the development of engineered constructs for bone fracture repair.

References

- [1] E. M. Kearney, E. Farrell, P. J. Prendergast, and V. A. Campbell, "Tensile strain as a regulator of mesenchymal stem cell osteogenesis." *Ann. Biomed. Eng.*, vol. 38, no. 5, pp. 1767–79, May 2010.
- [2] Y. F. Rui, P. P. Y. Lui, M. Ni, L. S. Chan, Y. W. Lee, and K. M. Chan, "Mechanical loading increased BMP-2 expression which promoted osteogenic differentiation of tendon-derived stem cells." *J Orthop Res*, vol. 29, no. 3, pp. 390–6, Mar. 2011.
- [3] G. Friedl, H. Schmidt, I. Rehak, G. Kostner, K. Schauenstein, and R. Windhager, "Undifferentiated human mesenchymal stem cells (hMSCs) are highly sensitive to mechanical strain: transcriptionally controlled early osteo-chondrogenic response in vitro." *Osteoarthr. Cartil.*, vol. 15, no. 11, pp. 1293–300, Nov. 2007.
- [4] M. Jagodzinski et al., "Effects of cyclic longitudinal mechanical strain and dexamethasone on osteogenic differentiation of human bone marrow stromal cells." *Eur. Cells Mater.*, vol. 7, pp. 35–41, 2004.
- [5] X. Liu and P. Ma, "Polymeric scaffolds for bone tissue engineering." *Ann. Biomed. Eng.*, vol. 32, no. 3, pp. 477–86, 2004.
- [6] H. Shin, S. Jo, and A. G. Mikos, "Biomimetic materials for tissue engineering." *Biomaterials*, vol. 24, no. 24, pp. 4353–64, Nov. 2003.
- [7] K. S. Anseth, C. N. Bowman, and L. Brannon-Peppas, "Mechanical properties of hydrogels and their experimental determination." *Biomaterials*, vol. 17, no. 17, pp. 1647–57, 1996.
- [8] J. a Stammen, S. Williams, D. N. Ku, and R. E. Guldberg, "Mechanical properties of a novel PVA hydrogel in shear and unconfined compression." *Biomaterials*, vol. 22, no. 8, pp. 799–806, 2001.
- [9] M. Castilho, I. Pires, B. Gouveia, and J. Rodrigues, "Structural evaluation of scaffolds prototypes produced by three-dimensional printing." *Int. J. Adv. Manuf. Technol.*, vol. 56, no. 5–8, pp. 561–69, Feb. 2011.

- [10] G. Chen, T. Ushida, and T. Tateishi, "Scaffold Design for Tissue Engineering." *Macromol. Biosci.*, vol. 2, no. 2, pp. 67–77, 2002.
- [11] S. Santhanam, J. Liang, J. Struckhoff, P. D. Hamilton, and N. Ravi, "Biomimetic Hydrogel with Tunable Mechanical Properties for Vitreous Substitutes." *Acta Biomater.*, vol. 43, pp. 327–337, 2016.
- [12] V. Terraciano et al., "Differential response of adult and embryonic mesenchymal progenitor cells to mechanical compression in hydrogels." *Stem Cells*, vol. 25, pp. 2730–38, 2007.
- [13] A. J. Engler, S. Sen, H. L. Sweeney, and D. E. Discher, "Matrix Elasticity Directs Stem Cell Lineage Specification." *Cell*, vol. 126, no. 4, pp. 677–89, 2006.
- [14] H. F. Hildebrand, N. Blanchemain, G. Mayer, F. Chai, M. Lefebvre, and F. Boschin, "Surface coatings for biological activation and functionalization of medical devices." *Surf. Coatings Technol.*, vol. 200, no. 22–23, pp. 6318–6324, Jun. 2006.
- [15] A. Sittichokechaiwut, A. M. Scutt, A. J. Ryan, L. F. Bonewald, and G. C. Reilly, "Use of rapidly mineralising osteoblasts and short periods of mechanical loading to accelerate matrix maturation in 3D scaffolds." *Bone*, vol. 44, no. 5, pp. 822–9, May 2009.
- [16] Z. Li, S. Yao, M. Alini, and M. J. Stoddart, "Chondrogenesis of human bone marrow mesenchymal stem cells in fibrin-polyurethane composites is modulated by frequency and amplitude of dynamic compression and shear stress." *Tissue Eng.*, vol. 16, no. 2, pp. 575–84, 2010.
- [17] S. H. Elder, S. A. Goldstein, J. H. Kimura, L. J. Soslowsky, and D. M. Spengler, "Chondrocyte differentiation is modulated by frequency and duration of cyclic compressive loading" *Ann. Biomed. Eng.*, vol. 29, no. 6, pp. 476–82, 2001.
- [18] S. D. Thorpe, T. Nagel, S. F. Carroll, and D. J. Kelly, "Modulating gradients in regulatory signals within mesenchymal stem cell seeded hydrogels: a novel strategy to engineer zonal articular cartilage." *PLoS One*, vol. 8, no. 4, pp. 60764–77, Jan. 2013.
- [19] R. M. Delaine-Smith and G. C. Reilly, "Mesenchymal stem cell responses to mechanical stimuli." *Muscles. Ligaments Tendons J.*, vol. 2, no. 3, pp. 169–80, 2012.
- [20] C. T. Rubin, K. J. McLeod, and S. D. Bain, "Functional strains and cortical bone adaptation: Epigenetic assurance of skeletal integrity." *J. Biomech.*, vol. 23, no. SUPPL. 1, pp. 43–54, 1990.
- [21] A. Sittichokechaiwut, J. H. Edwards, A. M. Scutt, and G. C. Reilly, "Short bouts of mechanical loading are as effective as dexamethasone at inducing matrix production by human bone marrow mesenchymal stem cells." *Eur. Cells Mater.*, vol. 20, pp. 45–57, 2010.
- [22] M. Brunelli, C. M. Perrault, and D. Lacroix, "Mechanical response of 3D Insert PCL to compression." *J. Mech. Behav. Biomed. Mater.*, vol. 65, pp. 478–489, 2017.
- [23] M. Brunelli, C. M. Perrault, and D. Lacroix, "Collagen degradation, distribution and cellular interaction in a novel 3D hybrid PCL/collagen gel scaffold." *Biomaterials*, p. submitted, 2016.
- [24] C. Karlsson et al., "Human embryonic stem cell-derived mesenchymal progenitors-Potential in regenerative medicine." *Stem Cell Res.*, vol. 3, no. 1, pp. 39–50, 2009.

- [25] G. M. de Peppo et al., "Human Embryonic Stem Cell-Derived Mesodermal Progenitors Display Substantially Increased Tissue Formation Compared to Human Mesenchymal Stem Cells Under Dynamic Culture Conditions in a Packed Bed/Column Bioreactor." *Tissue Eng. Part A*, vol. 19, no. 1–2, pp. 175–187, 2013.
- [26] F. Guilak, D. M. Cohen, B. T. Estes, J. M. Gimble, W. Liedtke, and C. S. Chen, "Control of Stem Cell Fate by Physical Interactions with the Extracellular Matrix." *Cell Stem Cell*, vol. 5, no. 1, pp. 17–26, 2009.
- [27] S. H. McBride and M. L. Knothe Tate, "Modulation of stem cell shape and fate A: the role of density and seeding protocol on nucleus shape and gene expression." *Tissue Eng. Part A*, vol. 14, no. 9, pp. 1561–72, 2008.
- [28] S. Damaraju, J. R. Matyas, D. E. Rancourt, and N. A. Duncan, "The Effect of Mechanical Stimulation on Mineralization in Differentiating Osteoblasts in Collagen-I Scaffolds." *Tissue Eng. Part A*, pp. 1–12, Jul. 2014.
- [29] J. R. Mauney et al., "Mechanical Stimulation Promotes Osteogenic Differentiation of Human Bone Marrow Stromal Cells on 3-D Partially Demineralized Bone Scaffolds In Vitro," *Calcif. Tissue Int.*, vol. 74, no. 5, pp. 458–68, May 2004.
- [30] M. C. Raff, "Social controls on cell survival and cell death," *Nature*, pp. 397–400, 1992.
- [31] M. Guo and B. Hay, "Cell proliferation and apoptosis," *Curr. Opin. Cell Biol.*, vol. 11, no. 6, pp. 745–752, 1999.
- [32] M. Hughes-Fulford and C.-F. Li, "The role of FGF-2 and BMP-2 in regulation of gene induction, cell proliferation and mineralization.," *J. Orthop. Surg. Res.*, vol. 6, no. 1, p. 8, 2011.
- [33] E. Baas, J. H. Kuiper, Y. Yang, M. A. Wood, and A. J. El Haj, "In vitro bone growth responds to local mechanical strain in three-dimensional polymer scaffolds," *J. Biomech.*, vol. 43, no. 4, pp. 733–739, 2010.
- [34] A. O. Duty, "Cyclic Mechanical Compression Increases Mineralization of Cell-Seeded Polymer Scaffolds In Vivo," *J. Biomech. Eng.*, vol. 129, no. 4, p. 531, 2007.
- [35] A. Roshan-Ghias, A. Terrier, P. E. Bourban, and D. P. Pioletti, "In vivo cyclic loading as a potent stimulatory signal for bone formation inside tissue engineering scaffolds," *Eur. Cells Mater.*, vol. 19, pp. 41–49, 2010.
- [36] S. D. Thorpe, C. T. Buckley, T. Vinardell, F. J. O'Brien, V. Campbell, and D. J. Kelly, "The response of bone marrow-derived mesenchymal stem cells to dynamic compression following TGF-beta3 induced chondrogenic differentiation.," *Ann. Biomed. Eng.*, vol. 38, no. 9, pp. 2896–909, Sep. 2010.
- [37] A. Castro and D. Lacroix, "Response of PCL scaffolds to mechanical compression: a computational model," not Publ., 2015.

[38] S. D. Thorpe, C. T. Buckley, T. Vinardell, F. J. O'Brien, V. A. Campbell, and D. J. Kelly, "Dynamic compression can inhibit chondrogenesis of mesenchymal stem cells," *Biochem. Biophys. Res. Commun.*, vol. 377, no. 2, pp. 458–62, 2008.

[39] S. M. Tanaka, J. Li, R. L. Duncan, H. Yokota, D. B. Burr, and C. H. Turner, "Effects of broad frequency vibration on cultured osteoblasts.," *J. Biomech.*, vol. 36, no. 1, pp. 73–80, 2003.

Fig.1: Electroforce biodynamic chamber embedding shafts and filled with culture media (pink) for mechanical compression of samples.

Fig. 2: Cyclic compression of samples with superimposed initial ramp at 5% strain.

Fig.3: Schematic representation of the experiment. Samples were kept in culture for 28 days. Time points were set at day 1, 3, 7, 14, 21 and 28. At the time of the first two time points, samples were all non-loaded, so just three samples were tested for DNA and OCN expression, and μ CT. The following two time points match the period of the first series of compression. So at day 7 and 14, six samples, three non-loaded and as many loaded, were tested. As the second series of stimuli was applied between day 16 and 20, three more samples were tested at the last two time points to account simultaneously for U, L1 and L2.

Fig. 4: 2D slides obtained from reconstruction of microCT images. (A) 3D PCL cultured with cells after 28 days in culture. (B) Tissue (green) and (C) mineral (red) were selected through the structure by the FloodFill feature provided by Simpleware considering grey values between 3500-7500 for tissue and 13000-60000 for mineral.

Fig. 5: Viability of cells ($n = \text{mean} \pm \text{S.D.}$) by Presto Blue measurement over 28 days considering non-loaded (U), loaded once (L1) and twice loaded (L2) samples as average of three experiments. Stars highlight significant differences with $p < 0.05$ referring to * all the series or * just U samples.

Fig. 6: Fluorescent images of samples seeded with hES-MPs at 10X. Viable cells are green, while scaffold fibers are blue due to auto-fluorescent properties of PCL. At day 28 loaded samples show cells randomly oriented with a star-like shape.

Fig. 7: Cell number ($n = \text{mean} \pm \text{S.D.}$) over time for non-loaded (U), loaded once (L1) and twice loaded (L2) over 28 days. Samples from different groups were considered the same as at day 1 and day 3, as no statistical differences were found comparing metabolism of U, L1 and L2 by Presto Blue. Due to the ANOVA results on Presto blue assay, loaded (L1 and L2) samples at day 7 and day 14 were also considered as belonging to the same group. As a consequence, the amount of cells attributed to L1 for those two time points was simultaneously representative for the behaviour of L1 and L2. Significant differences are underlined: $*p < 0.05$.

Fig. 8: Volume of tissue ($n = \text{mean} \pm \text{S.D.}$) accounting for cells and ECM content considering GV ranging between 3,500 and 7,500 ($*p < 0.05$).

Fig. 9: internal (IN) and superficial (OUT) amount of tissue ($n = \text{mean} \pm \text{S.D.}$) quantified by μ CT scanning of non-loaded (U), loaded once (L1) and twice loaded (L2) samples over 28 days ($*p < 0.05$).

Fig. 10: Overall volume of mineral ($n = \text{mean} \pm \text{S.D.}$) detected by μCT for non-loaded (U), loaded once (L1) and twice loaded (L2) samples over 28 days, and referring to GV in a range between 13,000 and 60,000.

Fig. 11: internal (IN) and superficial (OUT) amount of mineral ($n = \text{mean} \pm \text{S.D.}$) quantified by μCT scanning of non-loaded (U), loaded once (L1) and twice loaded (L2) samples over 28 days ($*p < 0.05$).

Fig. 12: OCN content ($n = \text{mean} \pm \text{S.D.}$) over time normalized over total cell number measured by DNA. The test was performed on six samples per time point, for non-loaded (U), loaded once (L1) and twice loaded (L2). Stars indicate significant differences among conditions at the same time point.

Fig. 13: Fluorescent imaging of scaffolds at day 21 for (A) unloaded (B) loaded once and (C) loaded twice scaffolds.

Fig. 14: Cellular (blue) and mineral (red) tissue growth over time for non-loaded (U) (left), loaded once (L1) (centre) and twice loaded (L2) (right).

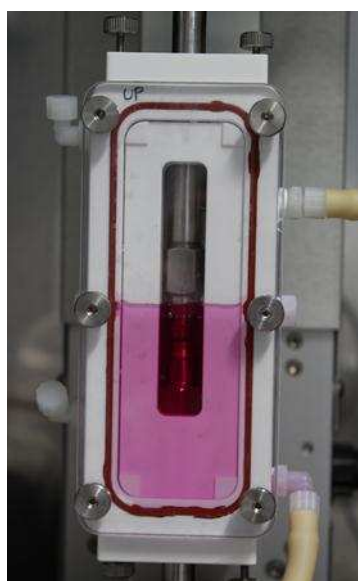


Fig. 1

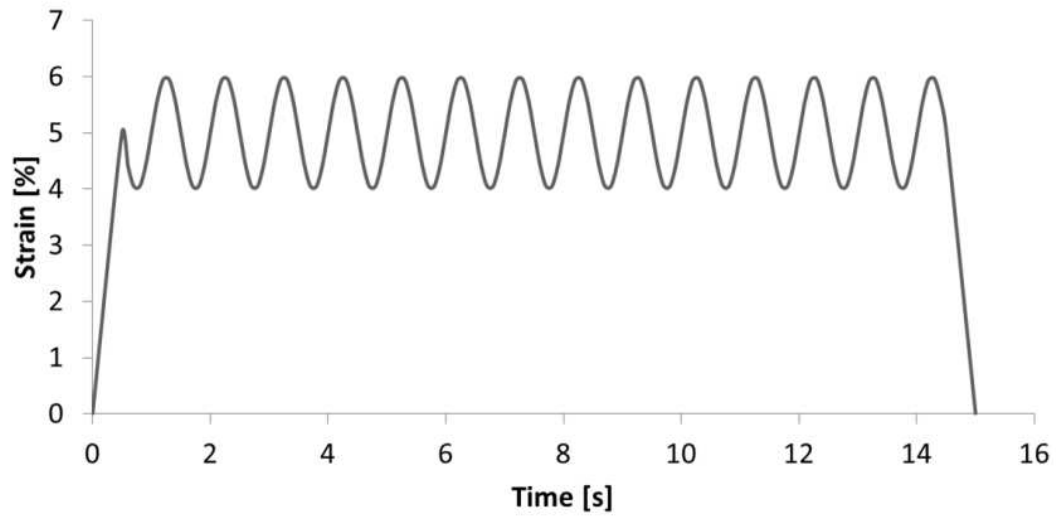


Fig. 2

Accepted manuscript

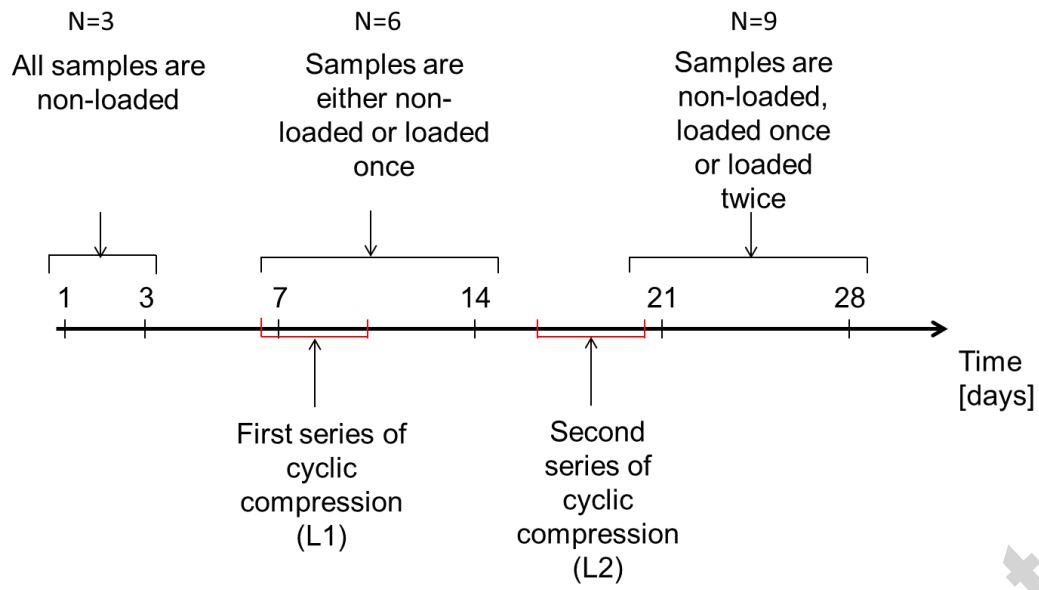


Fig. 3

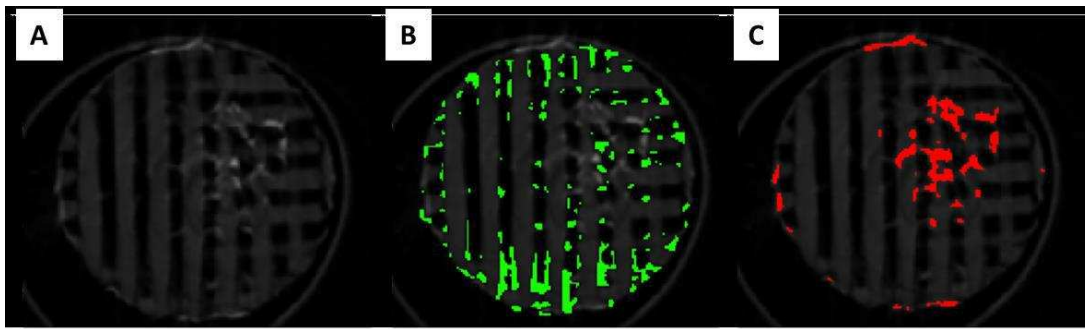


Fig. 4

Accepted manuscript

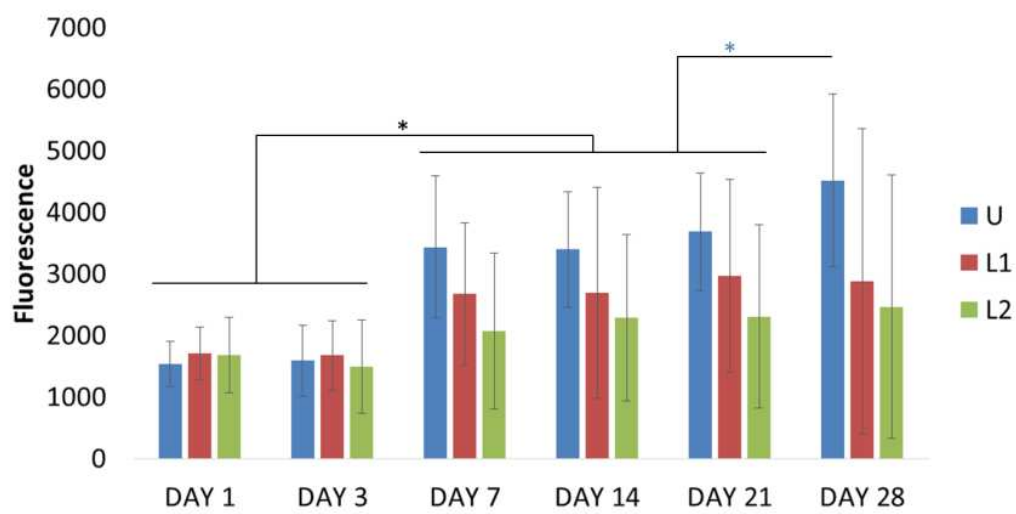


Fig. 5

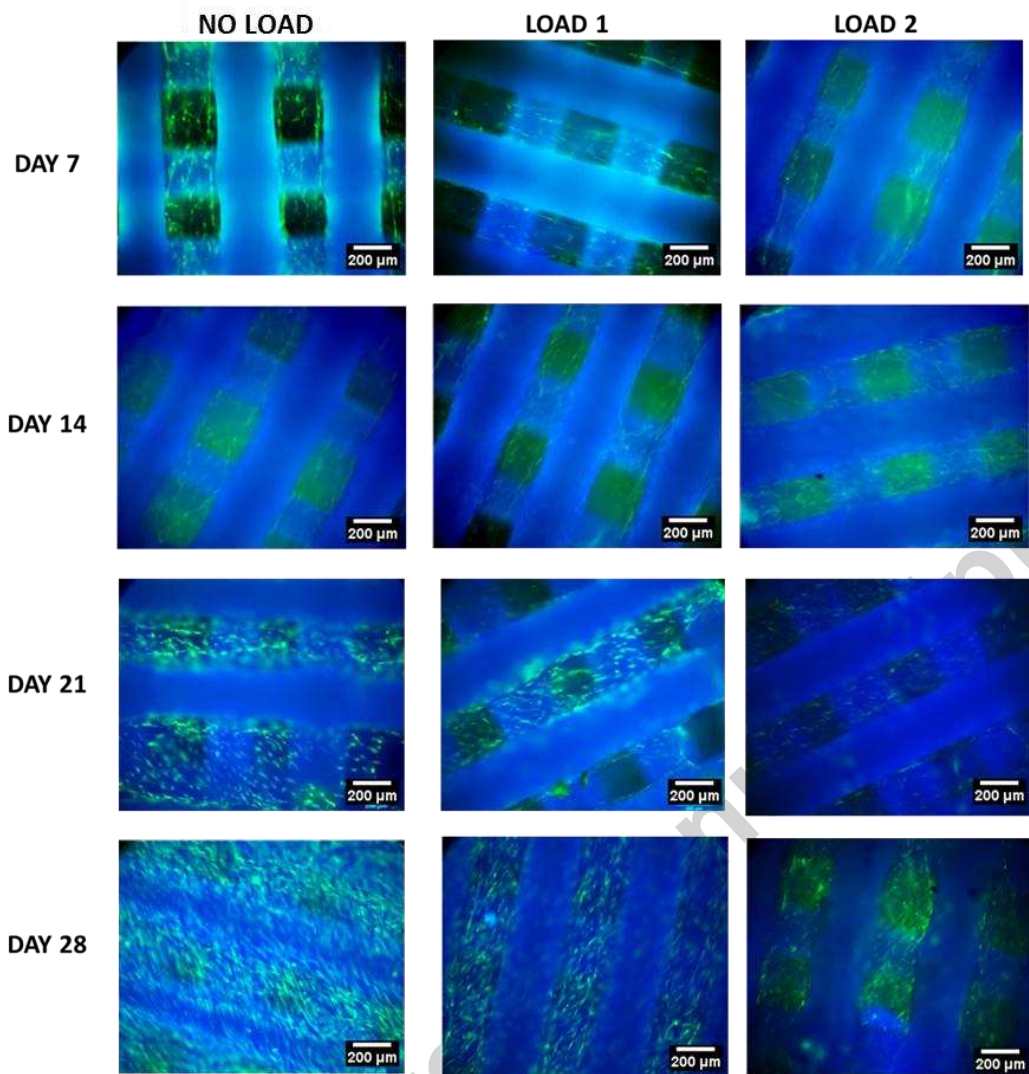


Fig. 6

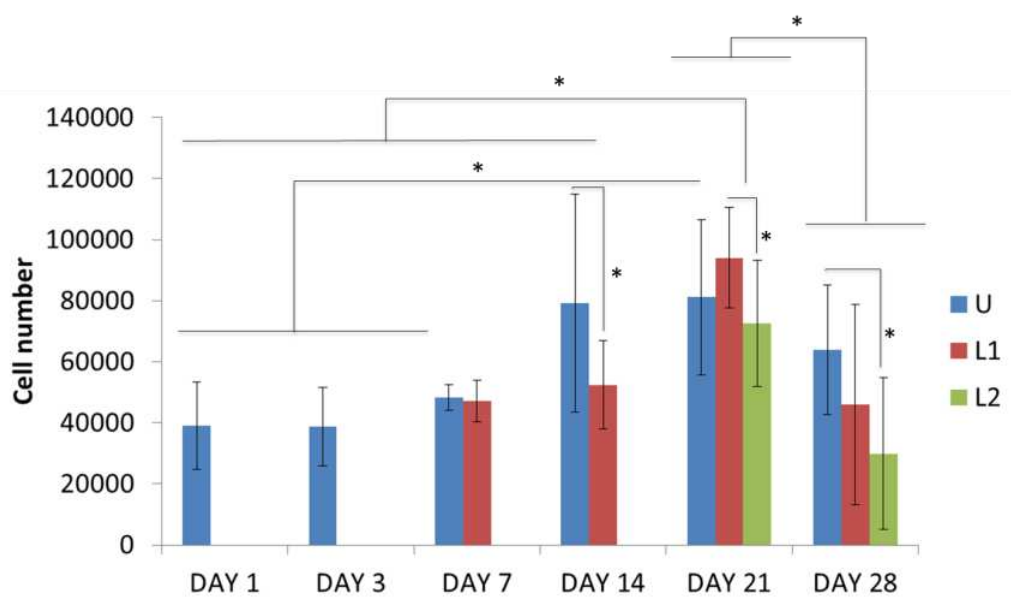


Fig. 7

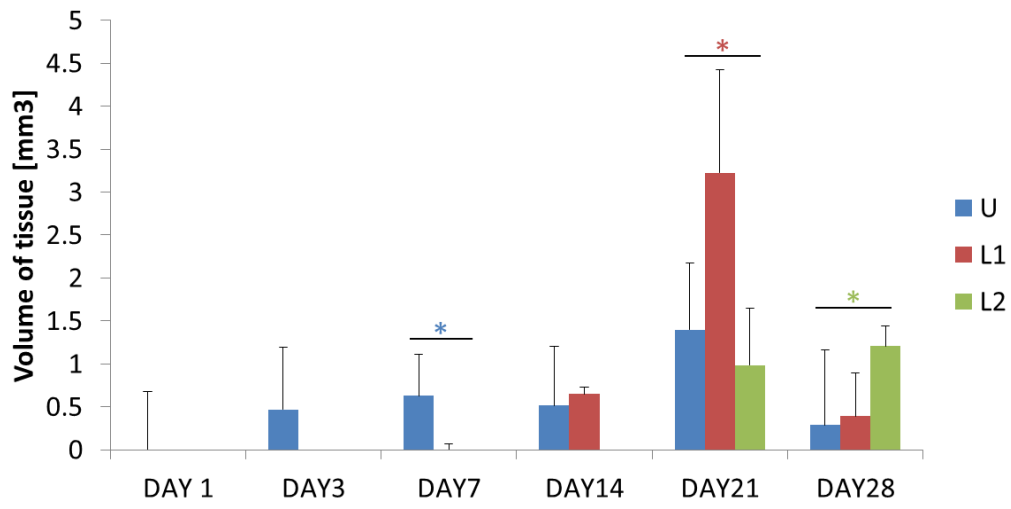


Fig. 8

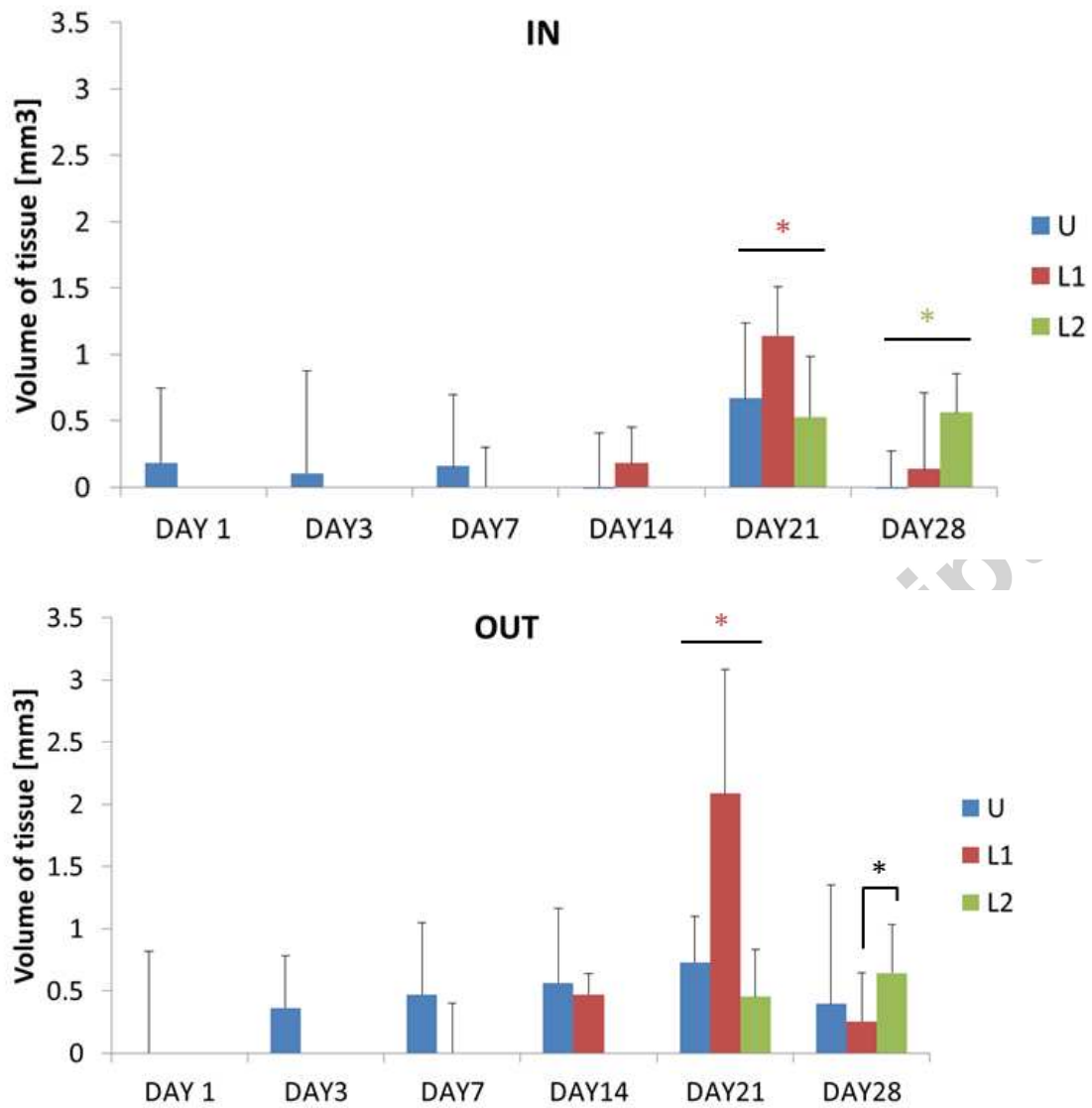


Fig. 9

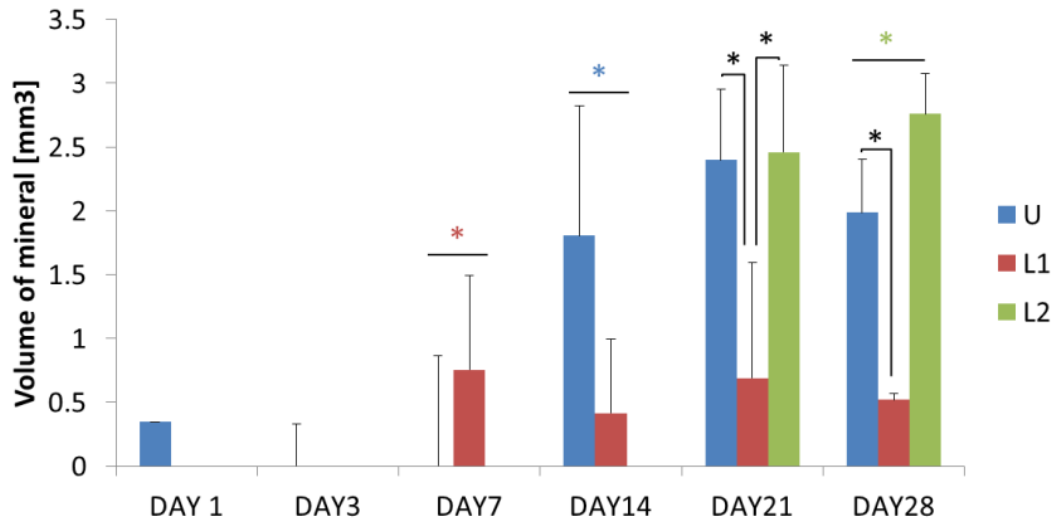


Fig. 10

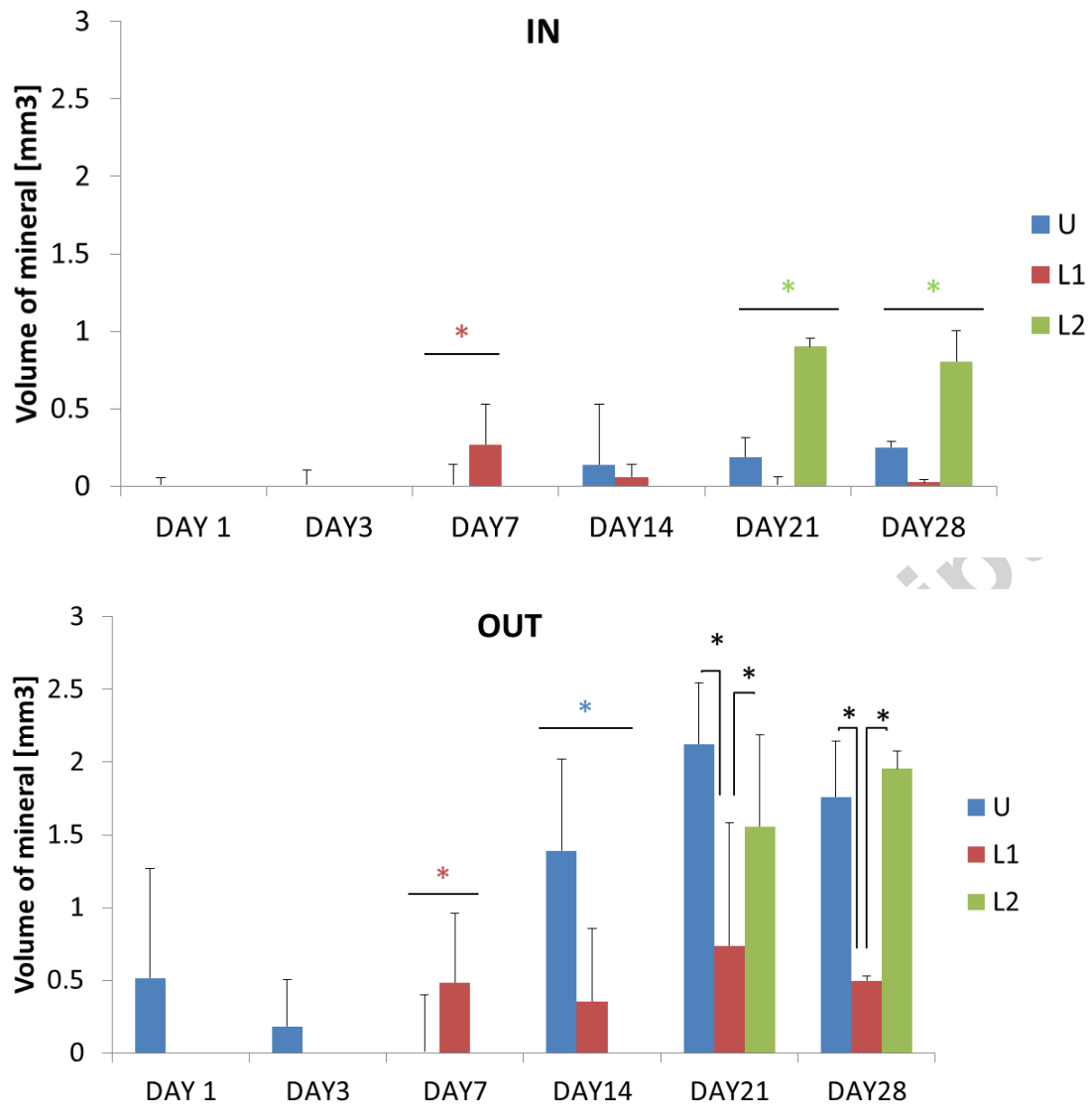


Fig. 11

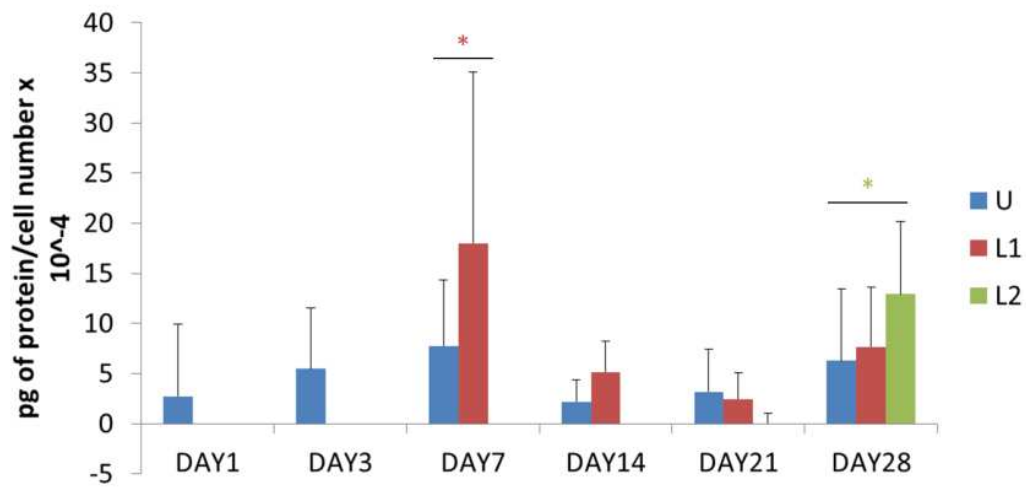


Fig. 12

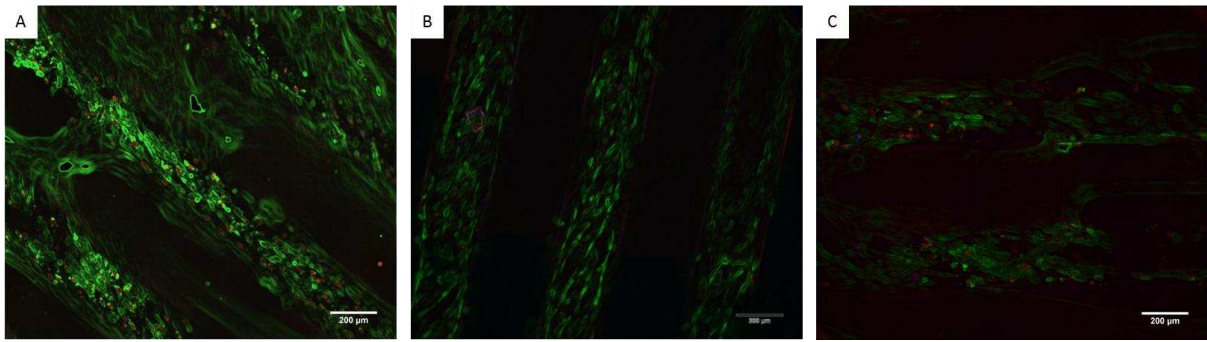


Fig. 13

Accepted manuscript

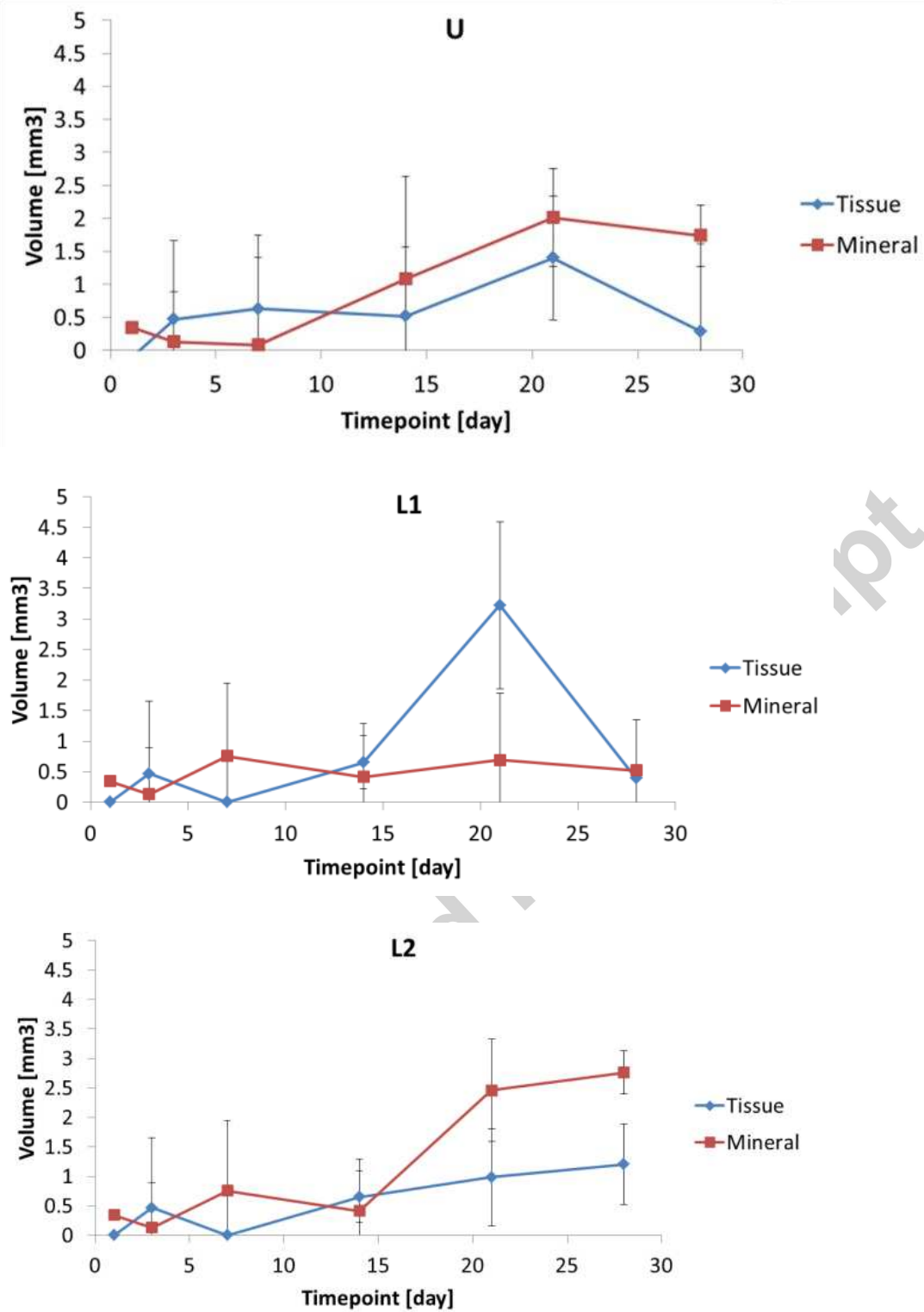


Fig. 14

Table 1: loading conditions applied to samples and total number of samples involved per each stimulation protocol. It is important to notice that non-loaded (U), loaded once (L1) and twice loaded (L2) samples were monitored respectively since day 1, day 7 and day 21.

CONDITION	ABBREVIATION	LOADING PROTOCOL	NUMBER OF SAMPLES
NO LOAD	U	-	18 (3x day 1,3,7,14,21,28)
LOAD 1	L1	From day 6 to day 10	12 (3x day 7,14,21,28)
LOAD 2	L2	From day 6 to day 10 and from day 16 to day 20	16 (3x day 21,28)

Table 2: Summary of the total number of samples used for DNA, OCN and μ CT analysis at each time point. The number of samples refers the total number of samples. So, the number of tested samples 1) at day 1 and 3 were three because all samples were non-loaded, 2) at day 7 and 14 were six to consider any difference caused by L1, and 3) at day 21 and 28 were nine to account for non-loaded (U), loaded once (L1) and twice loaded (L2).

TIMEPOINT TEST	TIMEPOINT	DAY 1	DAY 3	DAY 7	DAY 14	DAY 21	DAY 28
	CONDITION	U	U AND L1	U, L1 and L2			
DNA & OCN	NUMBER OF SAMPLES	6	6	12	12	18	18
	CTRL	3	3	3	3	3	3
MICROCT	NUMBER OF SAMPLES	3	3	6	6	9	9
	CTRL	3	3	3	3	3	3

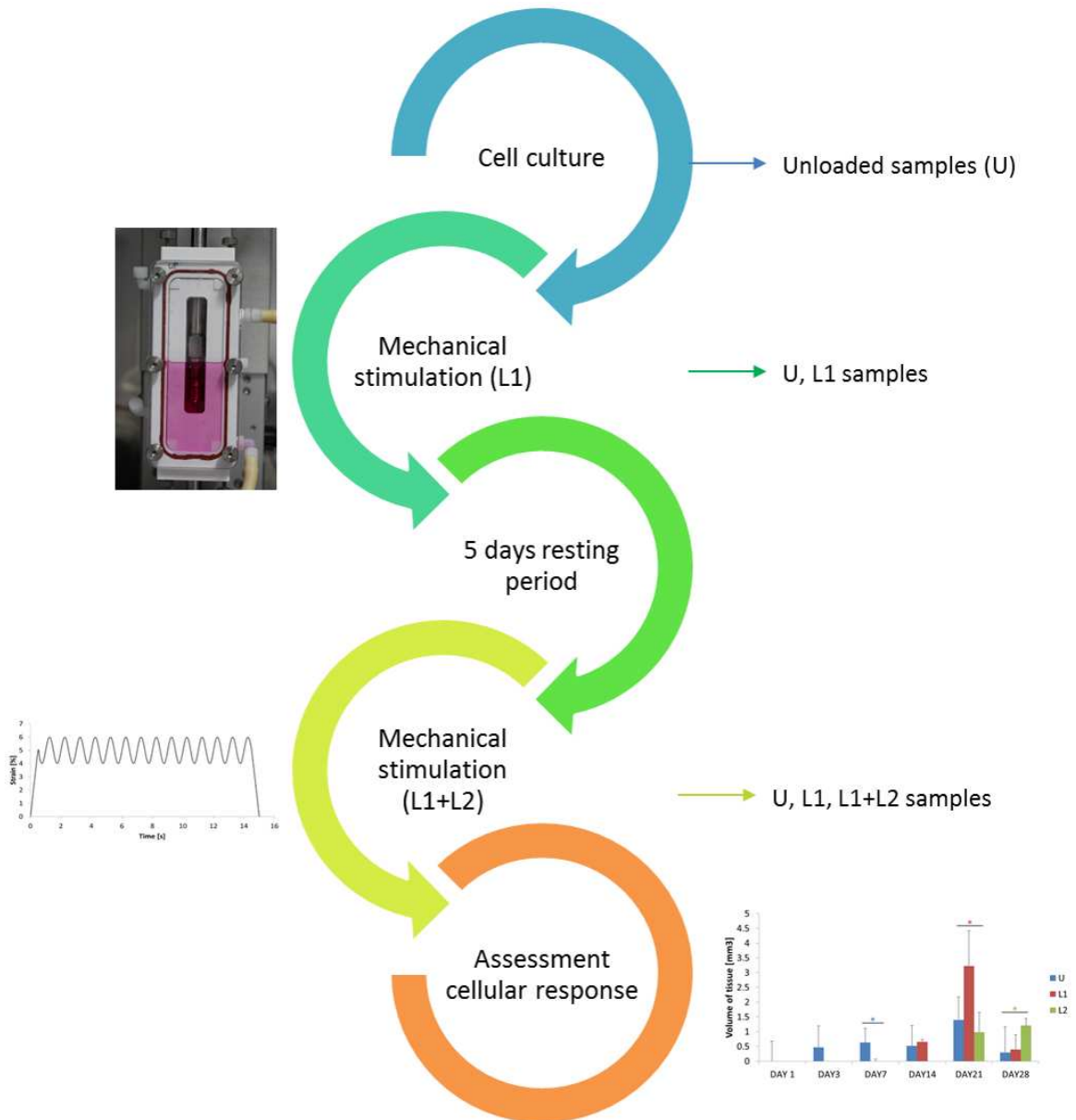
Table 3: Summary of the number of samples teste for metabolic activity by Presto Blue assays per each condition at each time point. The number indicates the total of samples tested in 3 different experiments.

TIMEPOINT CONDITION	DAY 1	DAY 3	DAY 7	DAY 14	DAY 21	DAY 28
NO LOAD	54	45	36	27	18	9

LOAD 1	36	36	36	27	18	9
LOAD 2	18	18	18	18	18	9
CTRL	36	30	24	18	12	6

Highlights

- Compression applied at early stage of culture delayed proliferation
- Compression applied at late stage of culture induced mineral deposition
- Repeated compression enhanced mineral deposition in the interior of scaffolds



ACCEPTED